Available online at www.sciencedirect.com

ScienceDirect

Energy Procedia 142 (2017) 253–258

Energy Procedia

www.elsevier.com/locate/procedia

9th International Conference on Applied Energy, ICAE2017, 21-24 August 2017, Cardiff, UK

A novel design of a rotary desiccant system for reduced dehumidification regeneration air temperature

Dominic O'Connor[a]*, John Kaiser Calautit[b] and Ben Richard Hughes[a]

[a]*Energy 2050, Faculty of Engineering, University of Sheffield, Sheffield, S102TN, United Kingdom*
[b]*Architecture and Built Env., University of Nottingham, Nottingham, NG72RD, United Kingdom*

Abstract

A novel design of rotary desiccant wheel has been tested experimentally in a two channel duct with countercurrent flow arrangement. Silica gel coated radial blades extending from the centre of the wheel were arranged at equally spaced intervals in 32-blade and 20-blade configurations. The design was focused on reducing the pressure drop across the device, as well as the regeneration temperature required for desorption of the desiccant compared to 80-120°C temperature currently required. It was envisioned that the increased air volume between radial blades would reduce the pressure drop and the regeneration temperature would be lowered due to the use of silica gel beads as compared to powder coating. The maximum pressure drop across the device was measured as 10.31Pa, significantly lower than current dehumidification systems. The regeneration air temperatures were set between 25°C and 40°C, increasing at 5°C increments. The experiments showed that reduction of the relative humidity of the airstream by up to 67% was possible within this range, whilst the silica gel continued to desorb water molecules, even at regeneration temperatures as low as 25°C. Further investigation with various parameter variables and designs will be undertaken to optimise the rotary desiccant wheel for low pressure drop and low regeneration air temperature.

Peer-review under responsibility of the scientific committee of the 9th International Conference on Applied Energy.

Keywords: dehumidification; desiccant material, rotary wheel; experimental testing

1. Introduction and Literature Review

Mechanical Heating, Ventilation and Air-Conditioning (HVAC) systems are amongst the most energy intensive systems used in buildings, requiring up to 40% of total energy consumption in UK buildings [1]. Lowering the

* Corresponding author. *E-mail address:* d.oconnor@sheffield.ac.uk

1876-6102
Peer-review under responsibility of the scientific committee of the 9th International Conference on Applied Energy .
10.1016/j.egypro.2017.12.040

energy demand of these systems would reduce the overall energy demand in buildings, and also have an impact on greenhouse gas emissions [2]. Rotary desiccant wheels can be used in HVAC systems to reduce the relative humidity in an incoming airstream through the adsorption of water molecules to the pore surface of a desiccant material, lowering the relative humidity. As the wheel rotates between the inlet and exhaust airstreams, the water molecules are desorbed from the pore surfaces by the high temperature of the exhaust, or regeneration, air. Typically this temperature is up to 120°C depending on the type of desiccant used, therefore additional energy costs are incurred to increase the regeneration air temperature to this level at which desorption can occur [3].
The development of new desiccant materials has shown that is it possible for the regeneration temperature to be lowered, results show 80°C is achievable [4]. However, these temperatures still require additional heat, and so energy, input for desorption. Further to this, the structure of a typical rotary desiccant wheel results in high pressure drop as high as 150Pa for airstreams. Fans are required to overcome this pressure drop to maintain air supply rates, incurring further energy costs [5]. A number of attempts have been made to lower the pressure drop associated with various heat recovery devices, which share similar principles as desiccant wheels, for integration with passive ventilation systems which require low pressure drop, by altering the configurations of the devices [6]. Significant reductions were possible, however the efficiency of the devices reduced as the pressure drop lowered due to the lower contact time between the air and the device [7].In order to address the high pressure drop and energy intensive regeneration air temperatures, a novel concept for a desiccant wheel was designed and tested experimentally. The results of this experimental testing are presented in this study to determine the effectiveness of the novel design in reducing the pressure drop and regeneration temperature required.

2. Experimental Testing: Design Configuration, Prototype and Experimental Setup

The aim of the novel design was to reduce the pressure drop of the airstream across the device, as well as reduce the regeneration temperature required for desorption. A previous attempt to redesign a rotary desiccant wheel was undertaken with a similar configuration of radial blades extending from the centre of the wheel outward [8,9]. Rapid prototyping using a 3D printer was used to construct the components of the rotary desiccant wheel using the process of Fused Deposition Modelling (FDM). The geometry of the prototype was designed using SolidWorks CAD (Computer Aided Design) software.

The prototype of the novel rotary desiccant wheel was assembled from separate components manufactured using a 3D printer. The wheel was printed in four quarters and inner and outer sections of the wheel were designed to fit together precisely, as shown in Figure 1A, the accuracy of the printer enabled this to be possible. The inner sections allowed for 20-blade and 32-blade configurations to be inserted into the design, held in place by the outer section. The geometry of the novel design was based on the maximum available dimensions (150x150x150mm in width x length x height directions respectively) of the printing bay of the printer.

The wheel featured an outer diameter of 300mm, including a toothed surface that allowed the wheel to be directly driven by a small geared motor at a constant angular velocity of 6rpm due to the fixed nature of the motor. This is higher than the common rotation speed of a desiccant wheel [10]. An inner diameter of 96mm was used to accommodate a shaft, about which the wheel could rotate freely. The wheel was 105mm deep to accommodate the radial blades and provide a secure hold.

The radial blades were 100x100x1mm in length, height and thickness respectively. In order for the blades to be held in position, 3mm deep slots were used in the inner wheel section, therefore the resulting area of the blades available was 94x100mm. The blades were made from acrylic plastic and coated with silica gel beads with an average diameter of 1mm. Acrylic was used at the material for the radial blades due to its inert properties with regard to low air temperatures and moisture. The final design of the prototype radial blade rotary desiccant wheel in the 20 blade configuration can be seen in Figure 1B. The rotary desiccant wheel was held in a printed casing to provide support and a rotation axis around a central shaft. The casing was located at the centre of ductwork featuring two separate channels to allow different inlet conditions to be achieved. The length of the ductwork was 490mm before and after the rotary wheel. Each separate channel of the ductwork had opening width and height dimensions of 160x325mm. The wall material thickness of the ductwork was 5mm for structural stability. The location of the rotary wheel inside the casing and ductwork can be seen in Figure 2.

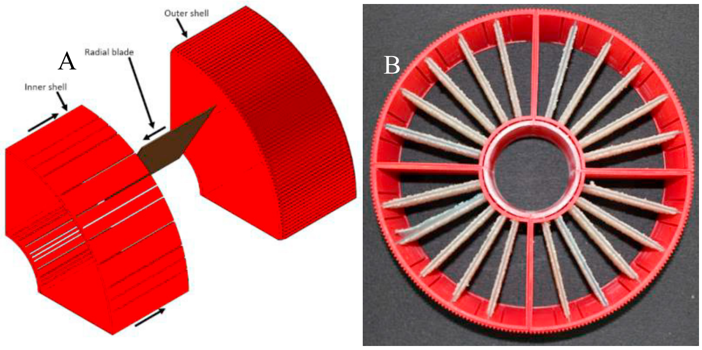

Figure 1 – A) CAD image of rotary desiccant wheel construction, B) Prototype rotary desiccant wheel with 20 radial blades

The flow through each of the channels of the ductwork was driven by two axial fans, mounted at the outlets of the channel to provide a suction force, drawing air from the inlet through the channel. This arrangement was found to have the profile most similar to the standard profile for flow in a duct. The incoming air inlet was open to the internal conditions of the laboratory. Air was fed from a managed source to the outgoing air inlet. A porous cloth material was added to inlets of the ductwork, as this was shown to improve the profile of the flow in the channels. The flow in the two ducts were arranged in a counter-current configuration, where the two directions of flow are in opposite directions. This is to better replicate the conditions commonly seen in ventilation systems. Though the channels of the ductwork were separated, cross contamination of the airstreams is possible given the design of the radial blades. As the wheel rotates, the gap between blades will span both airstreams. This allows the air from each channel to pass to the other channel, this is an unwanted consequence of the design. This renders the system unsuitable for situations where cross contamination is unacceptable.

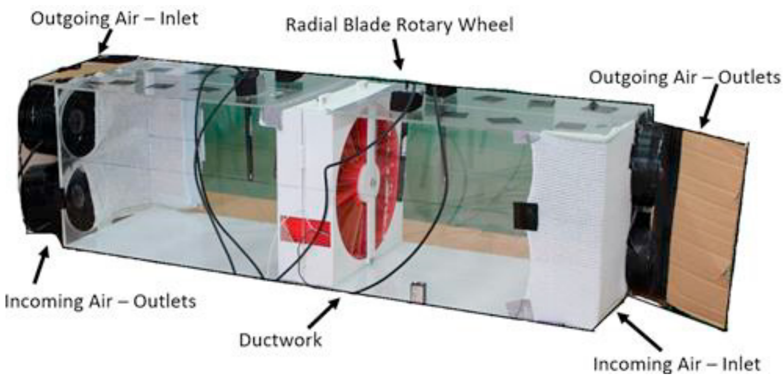

Figure 2 – Final experiment setup

The inlet conditions for the incoming and outgoing airstream were different to assess the performance of the rotary desiccant wheel. The inlet air temperature of the outgoing airstream was controlled by the temperature of an air heater which fed the inlet. The temperature was increased from 25°C to 40°C in 5°C intervals for both the 32-blade and 20-blade configurations. The relative humidity at the inlet of the outgoing airstream was measured between 12.5-29.4% depending on the air temperature. To increase the relative humidity of the inlet air of the incoming airstream to as close to 100% as possible, an ultrasonic humidifier was used to generate water vapour that was directed to the inlet of the incoming airstream. the poroues cloths improved the relative humidity distribution in the incoming air channel. The temperature of this inlet air was dependent on the ambient conditions of the laboratory and the relative humidity. This was measured between 13.6-17.4°C for the 32 and 20-blade configurations.Measurements for relative humidity and air temperature were taken before and after the rotary desiccant wheel in both the incoming and outgoing airstreams. Combined humidity and temperature probes were positioned 100mm upstream and downstream of the wheel, along the centreline of the channels at the mid-height. The probes were accurate to ±2%rH and ±0.3°C. Data loggers recorded the conditions of the air every 5 seconds for 1 hour, resulting in 720 measurements for each location. The measurement period was used to monitor the changes to the air over an extend timeframe as the changes to the air passing through the desiccant material would not be immediate. Measurements for air velocity were taken with a thermal anemometer before and after the rotary wheel, 100mm from each face along the centreline of each channel. The air velocity was measured at nine different heights to develop a flow profile along the height of the channel. The thermal anemometer was accurate to ±0.03m/s . The final experimental setup can be seen in Figure 2.

3. Results and Discussion

The velocity of air before and after the novel rotary desiccant wheel design was measured at nine different heights along the centreline of each channel, 100mm from each face of the wheel. The measurement results for the 32-blade and 20-blade configurations are shown in Figure 3. Incoming BW is the velocity profile in the incoming airstream before the wheel. Incoming AW is the velocity profile in the incoming airstream after the wheel. The profile of the flow before the wheel in both of the configurations, denoted by the blue trendlines, show that the flow profiles are similar to that of a fully developed flow in a duct. The flow velocity is lower close to the duct walls, reaching a maximum at the centre height. However, the measurements at 12cm above the centre height do not follow the expected trend, showing higher values than at the centre height. This is likely due to the suction driven flow caused by arrangement of the axial fans at the outlets. Furthermore, this height aligns with the height of the casing and wheel, whereby air may accelerate in the gap between the two components.

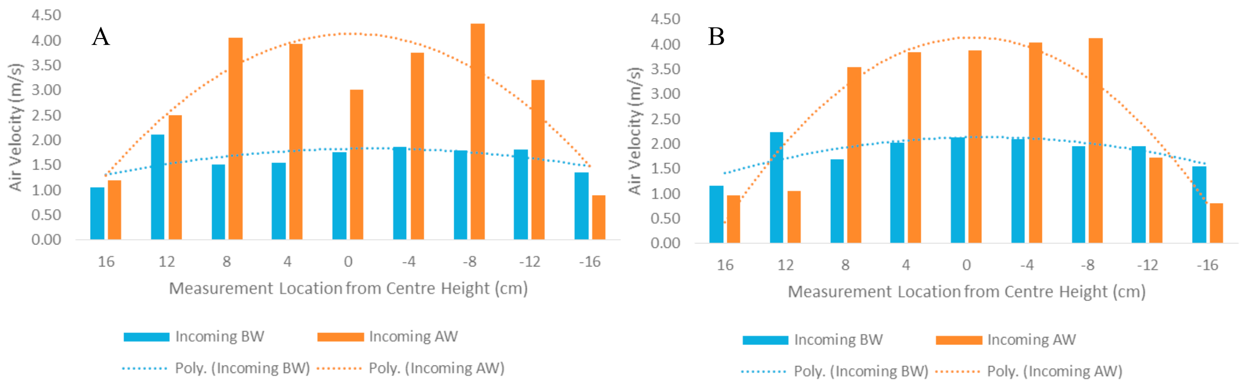

Figure 3 – Measurements of air velocity before and after rotary desiccant wheel A) 32 blade configuration, B) 20-blade configuration

The acceleration of the air through the rotary desiccant wheel is evident from the measurements of air velocity after the wheel, shown in orange. The increased air velocity after the rotary wheel in both configurations suggests that the volume contraction between the radial blades through which the air can flow, accelerates the air. The increased space between the radial blades allows for this effect to take place compared to the traditional design of a desiccant wheel. Though the air velocity trendlines after the rotary wheel suggest a fully developed flow, the measurements show that the flow did not behave completely as expected. Both configurations show measurement points with velocities higher than the centre height. Given the centre height of the channel aligns with the rotation shaft of the casing and the distance to the measurement point, it is likely that the wake caused by the rotation shaft results in the low air velocity at the centre height. The measured air velocities suggest that for the inlet velocity, adequate air can be supplied through the novel design of rotary desiccant wheel to provide ventilation for 17 occupants based on the recommendations of 8 litres per second per occupant [11].

The measurements for gauge pressure before and after the novel rotary desiccant wheel for the two radial blade configurations are shown, as the regeneration temperature of the outgoing airstream increased from 25°C to 40°C. The difference between the gauge pressure before and after the wheel was calculated as the pressure drop on the airstream in the configurations. The measurements for this are shown in Table 1. It is clear from the table that the regeneration air temperature has little effect on the gauge pressure value and hence little effect on the pressure drop. This is not unexpected given the low relative temperature difference between the tested conditions.

Table 1 - Measurements of gauge pressure before and after the novel rotary desiccant wheel in the 32 and 20-blade configurations

	32-blade			20-blade		
Regeneration Temperature	Before Wheel (Pa)	After Wheel (Pa)	Pressure Drop (Pa)	Before Wheel (Pa)	After Wheel (Pa)	Pressure Drop (Pa)
40°C	12.57	2.38	10.19	12.26	2.15	10.11
35°C	12.51	2.08	10.43	12.26	2.18	10.08
30°C	12.55	2.26	10.29	12.28	2.12	10.16
25°C	12.52	2.20	10.32	12.28	2.22	10.06

The average pressure drop for the 32-blade configuration is 10.31Pa and the average pressure drop for the 20-blade configuration is 10.08Pa. The 32-blade configuration has a higher pressure drop, as expected due to the increased number of blades and reduced space between blades, than the 20-blade configuration, though the difference is only 0.23Pa or 2.23%. This calculated pressure drop is significantly lower than the current pressure drop of 150Pa experienced by rotary desiccant systems. It is likely that this system would not require additional fans to provide ventilation supply rates, as previously shown. This would reduce the energy demand on systems utilising rotary desiccant wheels for dehumidification, thereby reducing greenhouse gas emissions.

The changes to relative humidity of the incoming and outgoing airstreams for the two radial blade configurations of the novel design of rotary desiccant wheel can be seen in Figure 4.

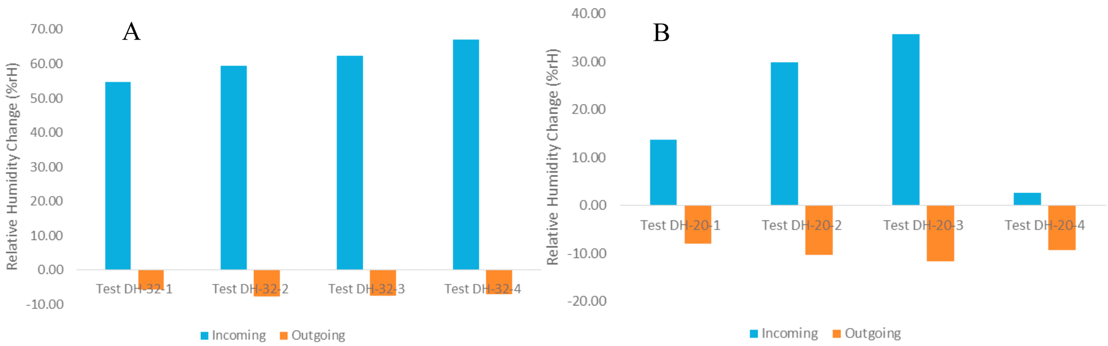

Figure 4 – Measurements of relative humidity change before and after rotary desiccant wheel in the incoming and outgoing airstreams A) 32 blade configuration, B) 20-blade configuration

The increase in outgoing air inlet temperature from 25°C to 40°C is shown as the tests increase from 1-4. A linear pattern exists in both configurations of radial blades, whereby the change in relative humidity of the incoming air increases as the outgoing air inlet temperature increases from 25°C to 40°C. This was the expected trend, as the temperature increases, water molecules are more easily desorbed from the pore surfaces of the silica gel beads. This results in the lower saturation of the silica gel, therefore a greater volume of water vapour can be adsorbed to the silica gel pores lowering the relative humidity by a greater value. The maximum decrease in relative humidity of 67% occurs in the 32-blade configuration at an outgoing air inlet temperature of 40°C. Given this was the configuration with the most number of blades, and hence silica gel volume, and highest outgoing air temperature, this is expected. The lowest relative humidity change in the incoming airstream was observed in the 20-blade configuration at an outgoing air inlet temperature of 40°C. The decrease of 2.6% is significantly lower than other values and is a surprising result given the high inlet temperature. The corresponding inlet relative humidity value for the incoming air was 63.5%, lower than the other tests. This was likely caused by experimental setup error and the cause of the lower change in relative humidity i.e. a lower volume of water vapour present in the air for adsorption.

As the outgoing air inlet temperature increases, the change in relative humidity of the outgoing air increases linearly. The maximum relative humidity change in the outgoing airstream of 11.6% was measured in the 20-blade configuration at an inlet temperature of 35°C. However, given the low incoming air relative humidity, it is likely that the 40°C inlet temperature test would produce the highest relative humidity increase based on the trend of the previous tests.

As the tests were conducted for one hour, the results from the experiments suggest that these effects are sustained over the duration of the testing period. The continuous regeneration of the silica gel at lower temperatures shows the potential for the novel design to lower energy costs. As no supplementary heating is required to raise the air temperature to the required value to desorb water molecules from the surface pores of the silica gel, waste heat from processes or exhaust air can be used for desorption.

4. Conclusion

A novel design for a rotary desiccant wheel was tested experimentally in a two channel ductwork. The design of the wheel used radial blades extending from the centre to the circumference in a regular arrangement of 32 or 20 equally spaced blades. The purpose of this design was to minimise the pressure drop across the wheel, and lower the required regeneration temperature for desorption. These effects would reduce the energy costs of the systems, and potentially enable the integration of this device into passive ventilation systems due to the low pressure drop.

The results of the experiment suggested the potential of the design to fulfill the aims for the device. The pressure drop across the device was measured as 10.31Pa and 10.08Pa for the 32 and 20-blade configurations respectively, significantly lower than current pressure drop values which can reach 150Pa. Analysis of the air velocity before and after the wheel showed that the wheel did not impede the air flow significantly, capable of supplying ventilation to 17 occupants are the tested inlet velocity. The relative humidity of the air was tested for the two configurations as the inlet air temperature for the outgoing airstream was increased from 25°C to 40°C in 5°C increments. The incoming air was dehumidified at all regeneration air temperatures tested. As expected, as the regeneration temperature increased the dehumidification of the air increased. The experiments showed that regeneration of the silica gel was possible at significantly lower temperatures than previously tested. Little to no additional energy would be required to raise the outgoing air temperature to the desired value for regeneration, thereby limiting the energy demand of the system. Further testing and exploration of the design and technology would enable optimisation with regards to configuration, material use and rotation speed.

Acknowledgements

The authors would like to acknowledge the support given by the Department of Mechanical Engineering at the University of Sheffield. The technology presented here is protected by international patent GB1506768.9.

References

[1] Parliament of the United Kingdom, 2010 to 2015 government policy: energy efficiency in buildings, 2015.
[2] Y. Fan, K. Ito, Energy consumption analysis intended for real office space with energy recovery ventilator by integrating BES and CFD approaches, Build. Environ. 52 (2012) 57–67. doi:10.1016/j.buildenv.2011.12.008.
[3] X.J. Zhang, Y.J. Dai, R.Z. Wang, A simulation study of heat and mass transfer in a honeycombed rotary desiccant dehumidifier, Appl. Therm. Eng. 23 (2003) 989–1003. doi:10.1016/S1359-4311(03)00047-4.
[4] N. Enteria, H. Yoshino, A. Satake, A. Mochida, R. Takaki, R. Yoshie, et al., Experimental heat and mass transfer of the separated and coupled rotating desiccant wheel and heat wheel, Exp. Therm. Fluid Sci. 34 (2010) 603–615. doi:10.1016/j.expthermflusci.2009.12.001.
[5] G. Angrisani, F. Minichiello, C. Roselli, M. Sasso, Experimental analysis on the dehumidification and thermal performance of a desiccant wheel, Appl. Energy. 92 (2012) 563–572. doi:10.1016/j.apenergy.2011.11.071.
[6] D. O'connor, J.K.S. Calautit, B.R. Hughes, A review of heat recovery technology for passive ventilation applications, Renew. Sustain. Energy Rev. 54 (2016) 1481–1493. doi:10.1016/j.rser.2015.10.039.
[7] A. Mardiana-Idayu, S.B. Riffat, Review on heat recovery technologies for building applications, Renew. Sustain. Energy Rev. 16 (2012) 1241–1255. doi:10.1016/j.rser.2011.09.026.
[8] D. O'Connor, J.K. Calautit, B.R. Hughes, A novel design of a desiccant rotary wheel for passive ventilation applications, Appl. Energy. 179 (2016) 99–109. doi:10.1016/j.apenergy.2016.06.029.
[9] D. O'Connor, J.K. Calautit, B.R. Hughes, A study of passive ventilation integrated with heat recovery, Energy Build. 82 (2014) 799–811. doi:10.1016/j.enbuild.2014.05.050.
[10] L.Z. Zhang, J.L. Niu, Performance comparisons of desiccant wheels for air dehumidification and enthalpy recovery, Appl. Therm. Eng. 22 (2002) 1347–1367.
[11] CIBSE, CIBSE Guide A: Environmental Design, 2015. doi:10.1016/0360-1323(94)00059-2.